Heating power at the substrate, electron temperature, and electron density in 2.45 GHz low-pressure microwave plasma

Abderrahmane Kais, Juslan Lo, Laurent P. Thérèse, Philippe Guillot

Physics of Plasmas

Heating power at the substrate, electron temperature, and electron density in 2.45 GHz low-pressure microwave plasma

Cite as: Phys. Plasmas **25**, 013504 (2018); https://doi.org/10.1063/1.5005592
Submitted: 19 September 2017 . Accepted: 18 December 2017 . Published Online: 08 January 2018

A. Kais, J. Lo, L. Thérèse, and Ph. Guillot

Heating power at the substrate, electron temperature, and electron density in 2.45 GHz low-pressure microwave plasma

A. Kais,[a),b)] J. Lo,[b)] L. Thérèse,[b)] and Ph. Guillot[b)]
Laboratoire Diagnostics des Plasmas Hors Equilibre, Université de Toulouse, INU Champollion, Place de Verdun, 81012 Albi cedex 9, France

(Received 19 September 2017; accepted 18 December 2017; published online 8 January 2018)

To control the temperature during a plasma treatment, an understanding of the link between the plasma parameters and the fundamental process responsible for the heating is required. In this work, the power supplied by the plasma onto the surface of a glass substrate is measured using the calorimetric method. It has been shown that the powers deposited by ions and electrons, and their recombination at the surface are the main contributions to the heating power. Each contribution is estimated according to the theory commonly used in the literature. Using the corona balance, the Modified Boltzmann Plot (MBP) is employed to determine the electron temperature. A correlation between the power deposited by the plasma and the results of the MBP has been established. This correlation has been used to estimate the electron number density independent of the Langmuir probe in considered conditions. *Published by AIP Publishing*. https://doi.org/10.1063/1.5005592

I. INTRODUCTION

Most of the plasma applications such as surface functionalization[1] or chemical[2] and biological decontamination[3,4] require a good knowledge of the surface temperature in order to control the process. For example, in the food industry,[5,6] the treatment of food at moderate temperature is essential to avoid package damages and organoleptic quality alterations.

The determination of the heating power by analyzing the time variations of the temperature during plasma-solid interaction is widely used in the literature. This method is suitable with different kinds of plasmas environments, especially in radio-frequency plasma.[7–10] In general, the calorimetric probes used for the purpose are based on metal materials, which can be biased allowing the control of particles influxes at the surface. In this work, a new application of this method is developed in the case of microwave (MW) plasma by using a glass substrate as a calorimetric probe at floating potential.

In the first part of this paper (Sec. III A), the experimental and theoretical methods used to determine the power contributions involved in the heating of the substrate surface will be described. The total power transferred from the plasma to the substrate is measured and calculated in a wide range of pressure and microwave (MW) power.

In Sec. III B, the modified Boltzmann plot is used to determine the electron temperatures. This method is based on Optical Emission Spectroscopy (OES) measurements and assumes that the upper energy levels of the atoms used for the investigation are close to a corona balance.

In the last part, a formula connecting the results of the modified Boltzmann plot to the heating power is established and implemented in order to estimate the electron number density. The results are compared to the measurements obtained by the Langmuir probe and the effect of the experimental conditions is shown and discussed.

II. EXPERIMENTAL SET-UP

Our experimental device consists of a vacuum chamber with a diameter of 56 cm and a height of 22 cm, Fig. 1(a). This study was carried-out in two different gas conditions, pure argon and argon-oxygen(10%) mixture, in a pressure range of 10 to 30 Pa. The plasma is generated by a coaxial microwave plasma source [*Hi-Wave Sairem*, Fig. 1(b)] which is powered by a 2.45 GHz Solid State Generator operating from 1 to 200 W. The reflected powers vary from 1 to 8 W. In the first part (Sec. III A), Langmuir probe (*Impedans Ltd.*) was used to measure plasma parameters such as electron energy distribution function (EEDF), electron number density n_e and electron temperature T_e. The temperature variation of the glass substrate was measured using a *K-type* thermocouple. OES measurements were performed using an *Avaspec 2048–2-Avantes* spectrometer with a 0.35 nm resolution.

III. EXPERIMENTAL RESULTS AND DISCUSSION

A. Heating power at the substrate

As it was briefly indicated in the introduction, the glass substrate acts as a temperature receptor. This thickness d, radius r, and specific heat capacity c_s are, respectively, equal to 2 mm, 5.5 cm, and 830 K kg^{-1} J^{-1}. The thermocouple is connected onto the substrate surface by means of a small and thin adhesive paper (autoclave indicator paper) representing 1% of the glass surface. It allows a good thermocouple-surface connection (see Fig. 2). The measurements are carried out through an electronic circuit permitting the cold-junction compensation and the reduction of measurement noises. The signals are processed by an NI-USB-6009 acquisition card and a Labview program.

[a)]Electronic mail: akais@univ-jfc.fr
[b)]URL: https://www.univ-jfc.fr/ea/diagnostic-des-plasmas-hors-equilibres-dphe-ea-4562.

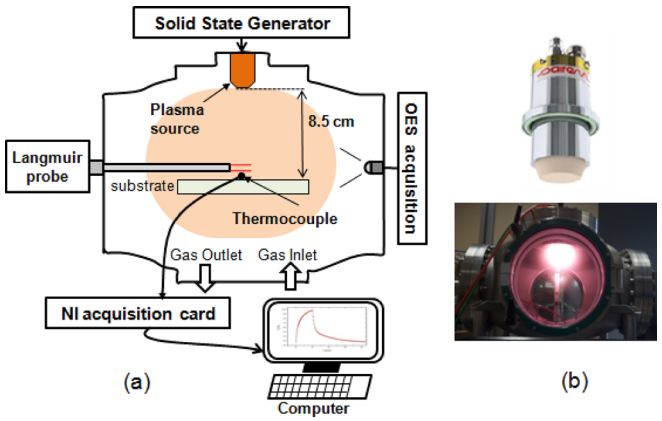

FIG. 1. (a) Schema of the vacuum chamber, diagnostic devices and (b) plasma source *Hi-Wave* (*Sairem* company) used in the study.

When the plasma is switched-on, the substrate will be heated during the time exposition. In this case, the power absorbed by the substrate P_s can be deduced from the first derivative function of the curve temperature using the following expression:

$$P_s = C_s \frac{dT_H}{dt}[W], \tag{1}$$

where $C_s = m_s\, c_s$, and T_H are the heat capacity and the measured temperature in the heating phase, respectively. m_s is the mass of the substrate and C_s is equal to 65 K J^{-1}.

In Fig. 2, different power components provided by the microwave generator are schematized. The power injected (P_g) is considered to be fully absorbed by the plasma. A part of this power is used for plasma sustaining purpose, while the remaining is dissipated through radiative and wall losses.

If we consider the power balance of the substrate, P_s is the part of the incoming power P_{in} which is responsible for the substrate temperature increase. The second part of P_{in} is released outside the substrate by radiation and thermal conduction with the gas and the holder. P_{out} can be determined by measuring the temperature variation in the plasma-off phase using the following relation:

$$P_{out} = -C_s \frac{dT_C}{dt}[W]. \tag{2}$$

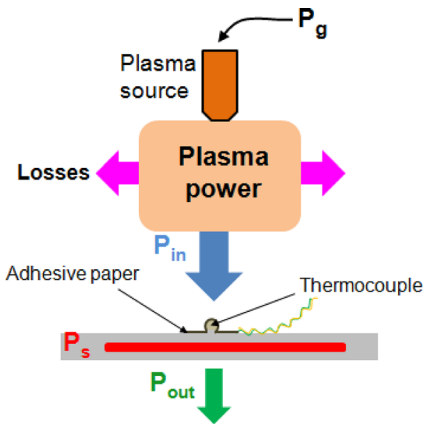

FIG. 2. Representation of the powers involved in the experimental device and the thermocouple-substrate connection.

In this work, we will focus on the input power coming from the plasma to the substrate P_{in} in order to link it to the plasma parameters. For this purpose, P_s and P_{out} are used and the following power balance at the substrate is established:[7,11]

$$P_{in} = P_s + P_{out} = C_S \times \left(\frac{dT_H}{dt} - \frac{dT_C}{dt}\right)_{T_{mean}}[W], \tag{3}$$

where T_{mean} is the average temperature between the heating and cooling phases (cf. Fig. 3).

In general, the total power influx at the substrate can be described by the sum of the contributions due to electrons J_e, ions J_{ion}, electron-ion recombination J_{recomb}, neutrals J_n, and photons J_{phot},[9,12]

$$J_{in} = J_e + J_{ion} + J_{recomb} + J_n + J_{phot}[\mathrm{Wm}^{-2}]. \tag{4}$$

In our conditions, the main heating process is essentially due to the plasma particle bombardment.[13] Therefore, the photon contribution can be neglected (equal to few μWcm^{-2}).[13] The contributions of the neutrals are limited, as there are no association and chemical reactions at the surface. The effect of secondary electron contribution is also neglected. Electron and ion contributions are due to the transfer of their kinetic energies to the surface. For a Maxwellian electron energy distribution, the electron contribution can be described by the product of the electron flux density at the surface j_e and the mean electron energy $2k_BT_e$, where k_B is the Boltzmann constant and T_e is the electron temperature[8,14]

$$P_e = n_e \sqrt{\frac{k_B T_e}{2\pi m_e}} \exp\left(\frac{e_0 V_{sh}}{k_B T_e}\right) \times 2kT_e \times A_s[W]. \tag{5}$$

In Eq. (5), m_e, e_0, V_{sh}, and A_s represent, respectively, the mass of electron, the elementary charge, the sheath potential, and the total substrate area. V_{sh} can be related to T_e by the following expression:[10,15] $V_{sh} = (k_BT_e/2e_0)\ln(M/2\pi m_e)$, where M is the ion mass.

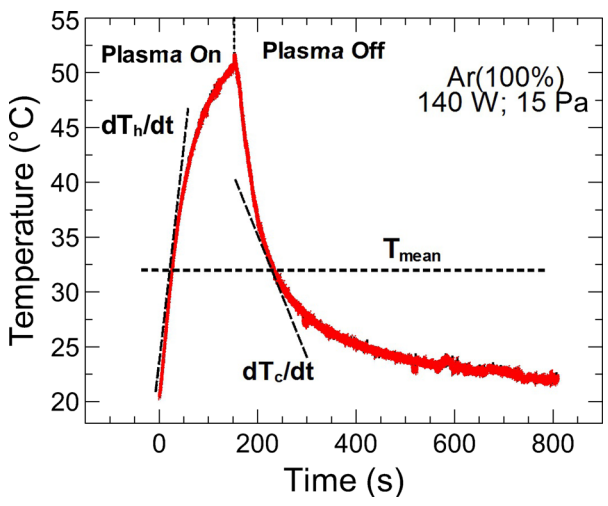

FIG. 3. $T_s(t)$ variations measured during the argon plasma exposition (15 *Pa*, 140 *W*, $T_{mean} = 32\,^{\circ}$C) and illustration of the method of P_{in} determination.

The contribution derived from the ion flux density j_{ion} to the surface is given by the product of the ion flux which overcomes the sheath and the ion energy at the sheath edge according to the Bohm criterion[16]

$$P_{ion} = 0.6 n_e \sqrt{\frac{k_B T_e}{M}} \times \frac{1}{2} k_B T_e \left[\left| \ln\left(\frac{2\pi m_e}{M}\right) \right| + 1 \right] \times A_s[W]. \tag{6}$$

Nevertheless, it should be noted that the mean electron energy used in Eq. (5) is only valid in the case of Maxwellian electron energy distribution function (EEDF). Indeed, if another type of EEDF holds, the electron heat contribution might differ. Kersten *et al.*[17] have studied the impact of EEDF (Maxwellian, Druyvesteyn, and monoenergetic distributions) on electron and ion contributions. One can see in their work that the influence of different EEDFs concerning P_e is negligible at the floating potential.

In our case, the EEDFs are measured using the Langmuir probe and compared to the theoretical Maxwellian and Druyvesteyn distributions. One can see in Fig. 4 that the electron energy distributions are very close to the Maxwellian function in the low energy range (below 11.5 eV corresponding to the excitation energy of argon) and slightly depleted in the high energy tail. This last observation can be explained by the large Ramsauer effect in argon as reported by Godyak and Piejak.[18] In the rest of this study, we assume that the EEDFs are close to Maxwellian distribution under the considered conditions.

According to Maurer[19] and Piejak *et al.*,[13] the contribution of the recombination term at the floating potential (j_e=j_{ion}) can be expressed using the ionization energy of the gas atoms E_{ion} (equal to 15.7 eV in the case of argon) and the electron flux density (j_e)

$$P_{recomb} = j_e E_{ion} \times A_s[W]. \tag{7}$$

Figure 5 shows the influence of the pressure on the different contributions calculated in argon plasma at 150 W. One can see that $P_{calcul} = P_e + P_{ion} + P_{recomb}$ is in good agreement with the powers determined from the temperature measurements using Eq. (3). Similar results are obtained in the case of the influence of the MW power represented in Fig. 6. One can observe that the electron-ion recombination is the dominant contribution to the heating. This occurrence is explained by the lowest kinetic energies of electrons and ions at floating potential. As shown in Eqs. (5) and (6), these energies are mainly influenced by the sheath potential (V_{sh}) which corresponds to the difference between the plasma potential and the surface potential. When V_{sh} changes (by applying a negative or positive potential at the substrate), the kinetic energy of the electrons and ions increases or decreases depending on the sign of the external potential. Under the conditions of this study, the substrate is maintained at the floating potential and the difference $Vp - Vf$ varies between 4 and 7 V (measured by the Langmuir probe). Note that similar results were obtained by Swinkels *et al.*[20] in argon plasma at comparable conditions.

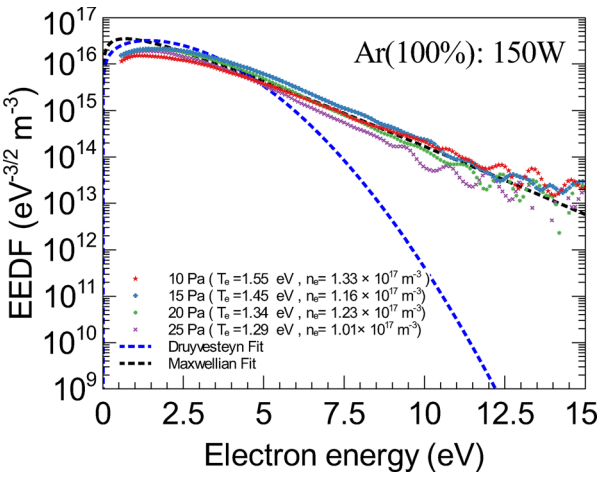

FIG. 4. Comparison of the EEDFs calculated from dI^2/dV^2 using Druyvesteyn formula with theoretical (Maxwellian and Druyvesteyn) distributions fits in pure argon plasma for different pressures at 150 W.

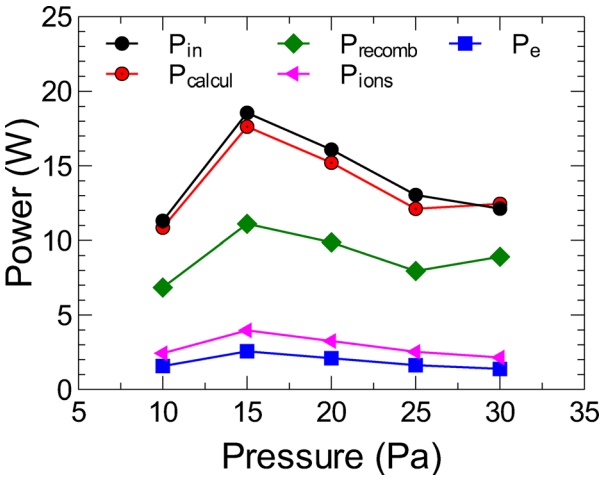

FIG. 5. Comparison of calculated and measured powers on the substrate surface in pure argon plasma for different gas pressures at 150 W.

Figure 6 shows that P_{in} increases linearly with increasing MW power supplied by the generator. This characteristic is generally known in low pressure plasmas under the same conditions.[21] The slope of the linear fitting of this feature corresponds to the power efficiency at 8.5 cm from the source and 15 Pa of pressure ($P_{in}/P_g = 12.40\% \pm 0.2$).

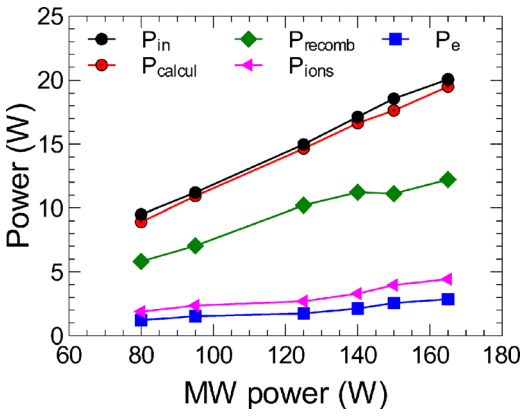

FIG. 6. Effect of MW power on the calculated and measured powers on the substrate surface in pure argon discharge at 15 Pa.

B. Determination of electron temperature using the modified Boltzmann plot

OES diagnostics are developed in order to determine the plasma parameters (Line-to-continuum ratio,[22] Laser scattering,[23] Boltzmann plot, etc.). In this work, the Boltzmann plot method is used in order to obtain the electron temperature T_e. For this purpose, eight excited states of the argon atom have been chosen as can be seen in the optical emission spectrum represented in Fig. 7.

In general, the conventional Boltzmann plot is used in the Local Thermodynamic Equilibrium (LTE) plasmas to determine the electron temperature.[24] In non-local-thermodynamic equilibrium (non-LTE) conditions, the temperature obtained by the conventional Boltzmann plot method corresponds to the excitation temperature T_{ex} which can be determined by inverting the slope of the following logarithmic function:[25]

$$ln\left(\frac{\lambda_{ij}I_{ij}}{A_{ij}g_i}\right) = \frac{-E_i}{k_B T_{ex}} + C, \tag{8}$$

where I_{ij} is the relative intensity of the emission line between the upper level i and the lower level j. λ_{ij}, g_i, A_{ij}, and E_i represent the wavelength (nm), the statistical weight, the transition probability for spontaneous radiative emission (in s^{-1}), and the excitation energy (eV) of the level i, respectively. k_B represents the Boltzmann constant and C is constant.

In our experiments, the LTE condition is not likely verified because of the small ionization degree and the low electron density of the plasma.[26] Consequently, the excitation temperature and the electron temperature will be different. Additionally, the considered excited states may not be completely governed by electronic collisions from the ground-state. According to Fujimoto,[26] in the low values of n_e (10^6–10^{11} cm^{-3}), 80% of populating mechanism is represented by the direct excitation from the ground-state level ($p = 1$), the rest of populating contributions comes from cascade from the highest energy levels ($p \geq 6$). In turn, the depopulation mechanism is controlled by radiative decay. In these conditions, the plasma can be governed by the corona balance which is expressed by the following formula:

$$n_i = \frac{n_1 n_e k_{1i}}{\sum_{i>j} A_{ij}}, \tag{9}$$

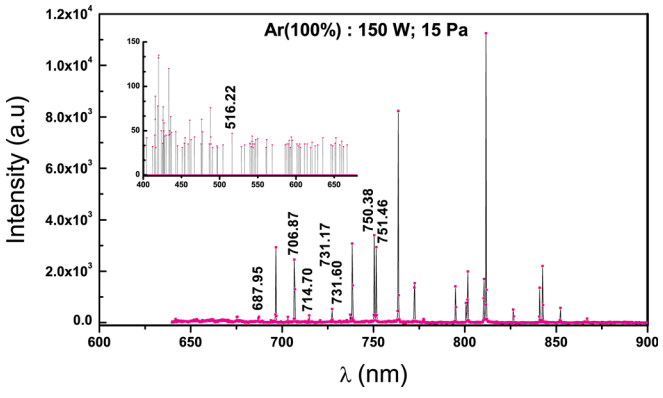

FIG. 7. Emission line spectrum in argon plasma at 150 W and 15 Pa.

where n_i and n_1 are the densities of the excited state population and the ground state level, respectively, and k_{1i} is the electron impact excitation rate coefficient from the ground state to the level i. In this case, it is necessary to modify the conventional Boltzmann plot to obtain the electron temperature. Before applying the modified Boltzmann plot, it is essential to ensure that our plasma is in the corona balance. To verify this, the effective principal quantum number[27] $p_i = \sqrt{\frac{E_H}{E_\infty - E_i}}$ (E_H is the Rydberg constant, E_∞ the ionization energy of the considered species and E_i the energy of the excited state i) was introduced and related to the relative population densities. The idea consists of representing the variation of the relative population densities of the considered levels i as function of p_i using the following expression:

$$ln\left(\frac{\lambda_{ij}I_{ij}}{A_{ij}g_i}\right) = -x \times ln(p_i) + Const. \tag{10}$$

Fujimoto[26] has demonstrated that the corona balance is satisfied when $0.5 \leq x \leq 6.0$, this range corresponds to the lower and upper electron density limits (10^6 for $x = 0.5$ and 10^{11} cm^{-3} for $x \simeq 6$) where the corona equilibrium takes place. For $x > 6$, the populating and de-populating processes are begin to change. In our conditions of pressure and microwave power, we have obtained $2.57 \leq x \leq 3.95$ for the emission lines considered. In view of this, we may conclude that our plasma fits the corona balance. Figure 8(b) shows an example of x determination in pure argon plasma at 15 Pa and 150 W. In Eq. (9), k_{1i} was obtained using the general expression in the case of argon discharge governed by Maxwellian electron energy distribution as follows:

$$\begin{aligned} k_{1i} = 8.69 \times 10^{-8} \times b_{1i} \times Z_{eff}^{-3} \times f_{1i} \times \left(\frac{(13.6 k_B T_e)^{2/3}}{(E_1 - E_i)/k_B T_e}\right) \\ \times \left(\frac{\exp[(E_1 - E_i)/k_B T_e]}{1 + (E_1 - E_i)/k_B T_e}\right) \\ \times \left[\left(\frac{1}{20 + (E_1 - E_i)/k_B T_e}\right) \right. \\ \left. + ln\left(1.25\left[1 + \frac{1}{(E_1 - E_i)/k_B T_e}\right]\right)\right], \end{aligned} \tag{11}$$

where b_{1i} is a constant with a value approximately equal to 1, $Z_{eff} = Z - N + 1 = 1$ is the effective atomic number, and Z and N are, respectively, the atomic number and the number of bound electrons. In order to evaluate the discrepancy from LTE and to take into account the corona balance, the conventional Boltzmann plot equation [Eq. (8)] may be modified by adding the parameter α_{1i},

$$ln\left(\frac{\lambda_{ij}I_{ij}\sum_{i>j}A_{ij}}{hc \times \alpha_{1i}A_{ij}}\right) = \frac{-E_{1i}}{k_B T_e} + D, \tag{12}$$

where $\sum_{i>j} A_{ij}$ represents the sum of the radiative transitions starting from the energy level considered, h is the Planck constant, c is the light velocity, and D is constant. This parameter was determined by fitting values of k_{1i} obtained

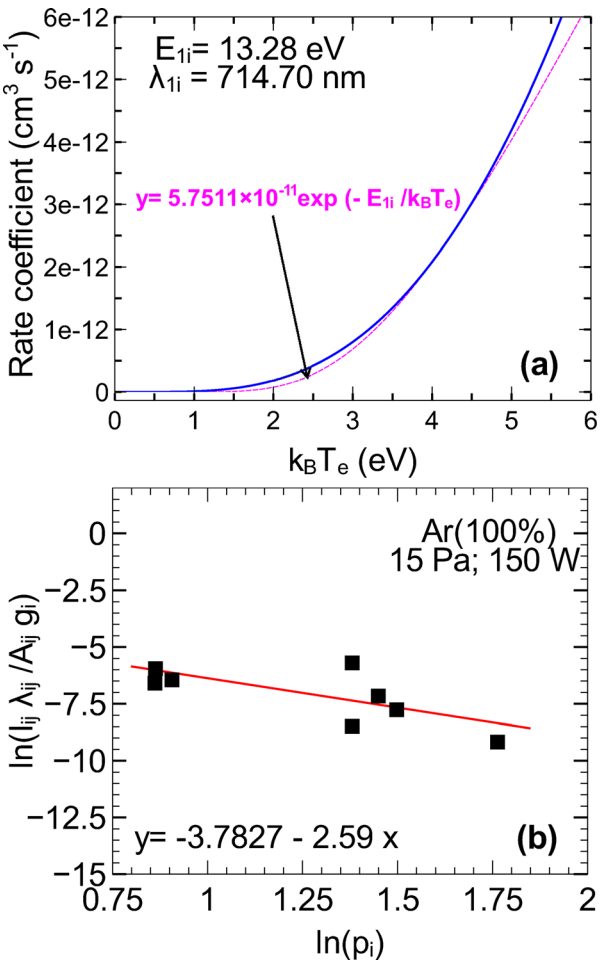

FIG. 8. Fitting function of k_{1i} [Eq.(13), dotted line] and its general expression [Eq. (11)], continuous line) in the case of argon (a). Relative population densities of the argon energy levels i used for this work as a function of their effective principal quantum number p_i in pure argon at 15 Pa; 150 W (b).

by Eq. (11) with the following exponential function depending on the electron temperature:

$$k_{1i} = \alpha_{1i} \times \exp\left(\frac{-E_{1i}}{kT_e}\right), \tag{13}$$

where α_{1i} is the coefficient of the exponential approximation of k_{1i} which depends on the product of E_{1i} (excitation energy of the level i) and p_i.[28] An example of the exponential fitting of the Eq. (11) from Eq. (13) is shown in Fig. 8(a), where values of k_{1i} for T_e ranging from 0.1 to 5 eV have been chosen for α_{1i} estimation in this work. In order to obtain the electron temperature, the best linear fitting was solved with Eq. (12) for all considered transitions listed in Table I.

Figure 9 shows a conventional and a modified Boltzmann plots corresponding to pure argon plasma at 15 Pa and 150 W. It is shown that the slope of the conventional Boltzmann plot is slightly higher than the one from the modified Boltzmann plot. This difference depends on the operating parameters (MW power, pressure, purity of the gas…). Although, in our case, T_{ex} is lower than T_e, under some experimental conditions, the adverse case is largely observed.[30] The main errors in obtaining the experimental data points used in the modified Boltzmann plot are inaccuracies in the determination of $\sum_{i>j} A_{ij}$ values; imprecise data in the recorded emission intensities and inaccuracies in the numerical fitting of the excitation rate coefficients k_{1i} allowing the determination of α_{1i}. Figure 10 shows the changes of T_e and T_{ex} as a function of pressure in pure argon discharge and argon with 10% of O_2. One can see that $T_{e(MBP)}$ decreases with increasing the pressure and tends to T_{ex} values. This effect may be assigned to the fact that the assumption of the corona balance does not take into account the distribution of high electron energy, as long as it considers only the excitation from the ground state. We can see that T_e in the case of pure argon plasma is higher than that of the Ar-O_2 plasma, this fact is also observed in comparable conditions by Chung *et al.*[30]

C. Determination of electron number density

The combination of calorimetric and Langmuir probes measurements is often used in the literature. In some published works, the authors use the calorimetric probe as electrostatic diagnostic to determine the plasma parameters using Langmuir probe theory.[31,32] Bornholdt and Kersten, have also combined the calorimetric method with Langmuir probe measurements. They discussed in their paper[8] the possible improvement of the calorimetric method in order to operate it at shorter measurement time and obtain additional information on the plasma. In this part, we will present an approach to determine the electron number density by combining the temperature-time variation

TABLE I. Spectroscopic data (λ_{ij}, E_i, g_i, A_{ij}, $\sum_{i>j} A_{ij}$) and fitting parameters α_{1i} corresponding to the considered transitions.

				α_{1i}			
λ_{ij} (nm)	E_i (eV)	g_i	A_{ij} (10^8 cm^3 s^{-1})	This work	Other authors	$\sum_{i>j} A_{ij}$(10^8 cm^3 s^{-1})	Transition
751.46	13.27	1	0.42900	2.5383×10^{-9}	3.307×10^{-9}[a]	0.428700[b]	4p → 4s
714.70	13.28	3	0.00643	5.7511×10^{-11}	6.500×10^{-11}[b]	0.006434 [b]	4p′ → 4s
750.38	13.48	1	0.74200	2.9026×10^{-9}	3.508×10^{-9}[a]	0.472400[b]	4p′ → 4s′
731.17	14.84	3	0.01770	4.1890×10^{-10}	2.552×10^{-10}[b]	0.055817[b]	6p → 4p
706.87	14.84	3	0.02000	7.9000×10^{-10}	…	0.051000[c]	4p → 4s
687.95	14.95	3	0.00180	5.6138×10^{-11}	…	0.007900[c]	4d → 4p
731.60	15.02	3	0.00960	2.3525×10^{-10}	…	0.015817[c]	6s → 4p
516.22	15.30	3	0.00914	1.1600×10^{-10}	5.859×10^{-11}[b]	0.031730[b]	6d → 4p

[a]From Ref. 27.
[b]From Ref. 28.
[c]Calculated from NIST data.[29]

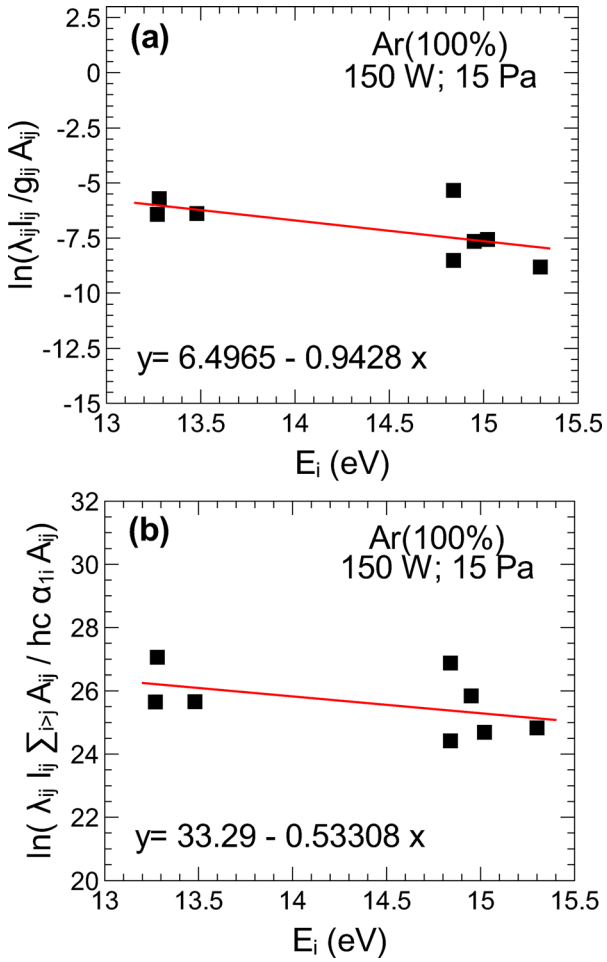

FIG. 9. Determination of the excitation temperature (a) using a conventional Boltzmann plot and the electron temperature and (b) using the modified Boltzmann plot in pure argon plasma at 15 Pa and 150 W (T_{ex}=1.10 eV, T_e=1.87 eV).

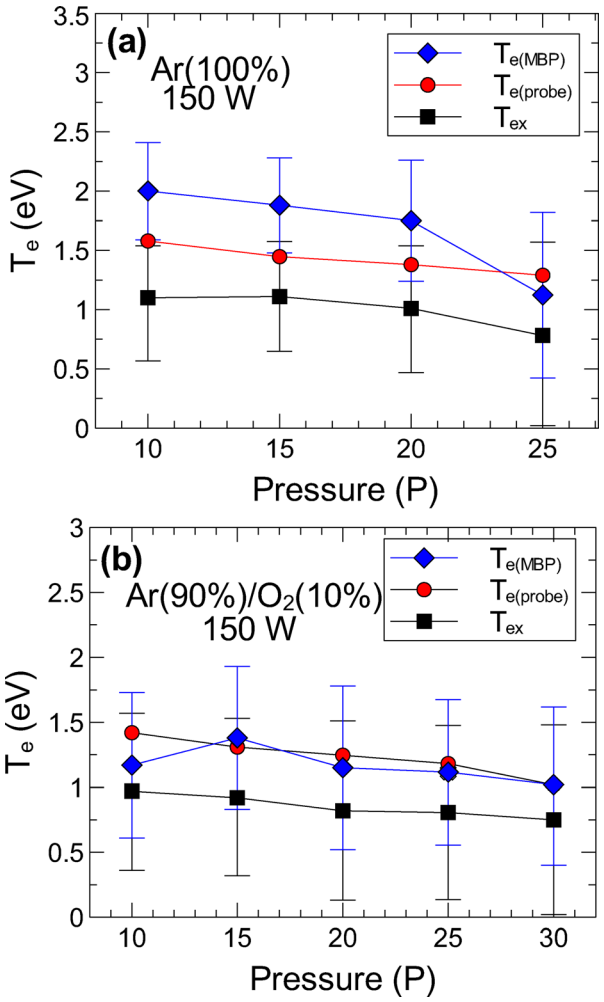

FIG. 10. Effect of the pressure on the excitation temperature and the electron temperatures measured by the Langmuir probe and obtained by a modified Boltzmann plot in pure argon (a) and in Ar(90%)/O_2(10%) and (b) at 150 W.

method with the Modified Boltzmann Plot (MBP) and Langmuir probe theory. This approach is based on the calculation of the input power at the substrate surface P_{in} [Eq. (3)] and the determination of the electron temperature using the modified Boltzmann plot. As shown previously, the input power at the surface is equal to the sum of electrons and ions contributions and their recombination at the substrate surface [Eqs. (5)–(7)]. One can see that these equations are only dependent on two unknown parameters, n_e and T_e. Therefore, one parameter knowledge allows the determination of the second. In our case, we will determine the electron density using the following expression:

$$n_e = \frac{P_{in}}{A_s}\left[\sqrt{\frac{k_B T_e}{2\pi m_e}}\exp\left(\frac{e_0 V_{sh}}{k_B T_e}\right)(2k_B T_e + E_{ion}) + 0.3k_B T_e\sqrt{\frac{k_B T_e}{M}}\frac{1}{2}k_B T_e\left|\ln\frac{2\pi m_e}{M} + 1\right|\right]^{-1}, \quad (14)$$

where E_{ion} is constant and V_{sh} is a function of T_e. The electron temperature data used in Eq. (14) are obtained from the modified Boltzmann plot method. Figure 11 shows the changes of electron number density versus the MW power and pressure variations. $n_{(probe)}$ and $n_{(calcul)}$ represent, respectively, the measurement values obtained from the Langmuir probe and calculated from Eq. (14). The results show a good agreement of $n_{e(probe)}$ and $n_{e(calcul)}$. One can also observe that both $n_{e(probe)}$ and $n_{e(calcul)}$ variations have the same tendencies compared to the P_{in} and P_{calcul} variations versus pressure and MW power obtained in the Sec. III A (Figs. 5 and 6). These changes are typical features of the plasma discharges under such conditions.[32]

It is important to report that the validity of the Eq. (14) depends greatly on the experimental conditions. The equality of the sum of the three contributions used in this study with the total power provided from the plasma may not be valid under some conditions, especially in plasmas where the contributions of negative ions, excited states, or neutral atoms are important. This fact would change the expression (14). The assumptions and important conditions of validity for this method are summarized as follows:

- Maxwellian EEDF distribution is verified in the considered conditions;
- the electron temperature used in Eq. (14) assumes that the plasma close to the corona balance;
- the glass substrate used as a calorimetric probe is at the floating potential;

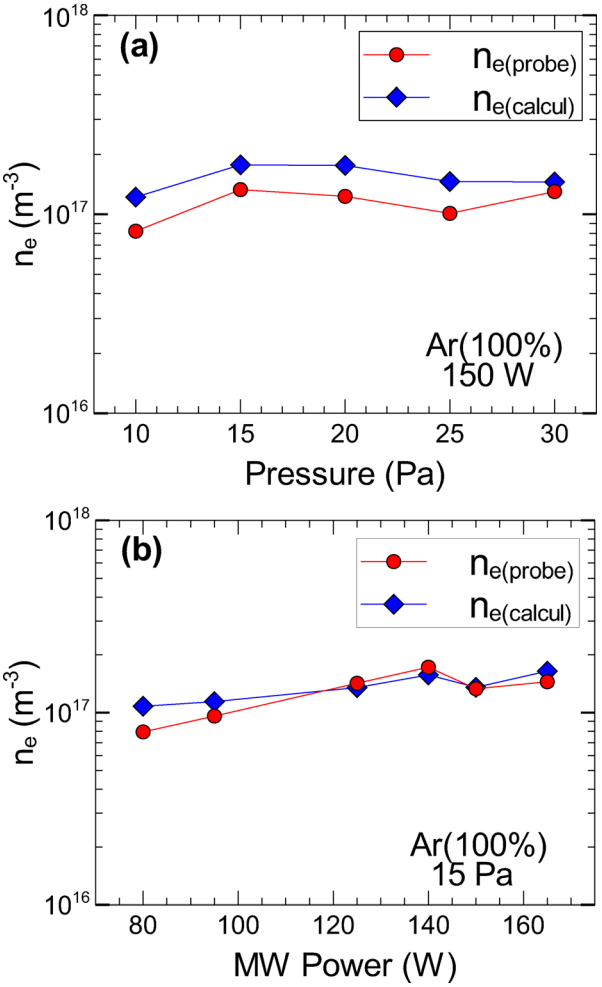

FIG. 11. Comparison of electron density calculated from Eq. (14) and measured by the Langmuir probe in pure argon plasma: (a) effect of the pressure at 150 W and (b) effect of MW power at 15 Pa.

- the main contribution to the heating power is due to the electron-ion recombination;
- the contribution of the photons to the heating power is neglected;
- the neutral contributions to the heating power are limited (association and chemical reactions at the surface are neglected);
- the effect of the of the secondary electrons on the power balance of the substrate is also neglected.

IV. CONCLUSION

In this study, we combined the calorimetric probe method, the Langmuir probe theory, and the modified Boltzmann plot in order to determine plasma parameters. First, the various contributions to the heating are calculated and the total power deposited onto the substrate is measured. It has been shown that the electron and ion influxes as well as their recombination at the substrate surface are the predominant contributions to the heating power.

Using the modified Boltzmann plot method and the corona equilibrium assumption, the electron temperature is determined in Ar and Ar-O_2 plasmas. The electron temperatures obtained by this method are in good agreement with the Langmuir probe measurements.

Finally, the combination of the calorimetric method and the modified Boltzmann plot is used to estimate the electron number density. This method is simple and less expensive than conventional methods. It can be adapted to various plasma environment and geometries, mainly in the case where using the Langmuir probe may be difficult because of its intrusive nature.

ACKNOWLEDGMENTS

The authors gratefully acknowledge the Midi-Pyrénées region for financial support.

[1]R. Gandhiraman, S. Karkari, S. Daniels, and B. McCraith, Surf. Coat. Technol. **203**, 3521 (2009).
[2]H. Herrmann, G. Selwyn, I. Henins, J. Park, M. Jeffery, and J. Williams, IEEE Trans. Plasma Sci. **30**, 1460 (2002).
[3]N. Ulbin-Figlewicz, A. Jarmoluk, and K. Marycz, Ann. Microbiol. **65**, 1537 (2015).
[4]K. Stapelmann, M. Fiebrandt, M. Raguse, P. Awakowicz, G. Reitz, and R. Moeller, Astrobiology **13**, 597 (2013).
[5]U. Schnabel, C. Schmidt, J. Stachowiak, A. Bösel, M. Andrasch, and J. Ehlbeck, Plasma Process Polym. **14**, e1600057 (2017).
[6]D. Purevdorj, N. Igura, I. Hayakawa, and O. Ariyada, J. Food Eng. **53**, 341 (2002).
[7]J. A. Thornton, Thin Solid Films **54**, 23 (1978).
[8]S. Bornholdt and H. Kersten, Eur. Phys. J. D **67**, 176 (2013).
[9]H. R. Maurer, M. Hannemann, R. Basner, and H. Kersten, Phys. Plasmas **17**, 113707 (2010).
[10]H. Kersten, E. Stoffels, W. W. Stoffels, M. Otte, C. Csambal, H. Deutsch, and R. Hippler, J. Appl. Phys. **87**, 3637 (2000).
[11]G. Makrinich and A. Fruchtman, J. Appl. Phys. **100**, 093302 (2006).
[12]H. Kersten, H. Deutsch, H. Steffen, G. Kroesen, and R. Hippler, Vacuum **63**, 385 (2001).
[13]R. Piejak, V. Godyak, B. Alexandrovich, and N. Tishchenko, Plasma Sources Sci. Technol. **7**, 590 (1998).
[14]H. Steffen, H. Kersten, and H. Wulff, J. Vac. Sci. Technol., A **12**, 2780 (1994).
[15]M. A. Lieberman and A. J. Lichtenberg, *Principles of Plasma Discharges and Materials Processing: Lieberman/Plasma 2e* (John Wiley & Sons, Inc., Hoboken, NJ, USA, 2005).
[16]P. Chabert and N. Braithwaite, *Physics of Radio-Frequency Plasmas* (Cambridge University Press, Cambridge, 2011).
[17]H. Kersten, G. Kroesen, and R. Hippler, Thin Solid Films **332**, 282 (1998).
[18]V. A. Godyak and R. B. Piejak, Phys. Rev. Lett. **65**, 996 (1992).
[19]H. Maurer, "Micro-particles as thermal probes in a low-pressure RF-discharge," Ph.D. thesis (Christian-Albrechts Universität Kiel, 2010).
[20]G. H. P. M. Swinkels, H. Kersten, H. Deutsch, and G. M. W. Kroesen, J. Appl. Phys. **88**, 1747 (2000).
[21]R. J. Visser, J. Vac. Sci. Technol., A **7**, 189 (1989).
[22]A. Sola, M. D. Calzada, and A. Gamero, J. Phys. D: Appl. Phys. **28**, 1099 (1995).
[23]T. Hori, M. D. Bowden, K. Uchino, K. Muraoka, and M. Maeda, J. Vac. Sci. Technol., A **14**, 144 (1996).
[24]W. Wiese, Spectrochim. Acta, Part B **46**, 831 (1991).
[25]M. Bashir, J. M. Rees, S. Bashir, and W. B. Zimmerman, Phys. Lett. A **378**, 2395 (2014).
[26]T. Fujimoto, J. Phys. Soc. Jpn. **54**, 2905 (1985).
[27]N. Tian-Ye, C. Jin-Xiang, L. Lei, L. Jin-Ying, W. Yan, W. Liang, and L. You, Chin. Phys. **16**, 2757 (2007).
[28]F. J. Gordillo-Vázquez, M. Camero, and C. Gómez-Aleixandre, Plasma Sources Sci. Technol. **15**, 42 (2006).
[29]"NIST: Atomic Spectra Database Lines Form."
[30]T. H. Chung, H. Ra Kang, and M. Keun Bae, Phys. Plasmas **19**, 113502 (2012).
[31]G. Golan and A. Axelevitch, Plasma Devices Operations **11**, 287 (2003).
[32]V. A. Godyak, R. B. Piejak, and B. M. Alexandrovich, Plasma Sources Sci. Technol. **1**, 36 (1992).